Journal of Alloys and Compounds 509 (2011) 7038–7041

Contents lists available at ScienceDirect

Journal of Alloys and Compounds

journal homepage: www.elsevier.com/locate/jallcom

Nanostructured $MgFe_2O_4$ as anode materials for lithium-ion batteries

N. Sivakumar[a], S.R.P. Gnanakan[a], K. Karthikeyan[b], S. Amaresh[b], W.S. Yoon[c], G.J. Park[d], Y.S. Lee[a,b,*]

[a] The Research Institute for Catalysis, Chonnam National University, Gwang-ju 500-757, Republic of Korea
[b] Faculty of Applied Chemical Engineering, Chonnam National University, Gwang-ju 500-757, Republic of Korea
[c] School of Advanced Materials Engineering, Kookmin University, Seoul 136-702, Republic of Korea
[d] Department of Applied Chemistry, Saga University, 1 honjo, Saga 840-8502, Japan

ARTICLE INFO

Article history:
Received 30 November 2010
Received in revised form 15 March 2011
Accepted 19 March 2011
Available online 29 March 2011

Keywords:
Lithium batteries
Anode material
$MgFe_2O_4$
Anomalous capacity

ABSTRACT

Transition metal oxides in the nano size region are enormous attention as a new generation of anode materials for high energy density Li-ion batteries. $MgFe_2O_4$ is used for the first time as active electrode vs. lithium metal in test cells. The research has been focused on the effect of grain size of $MgFe_2O_4$ and their electrochemical performance studied. In this studies, nanostructured milled $MgFe_2O_4$ (grain size 19 nm) sample have been compared with relatively large-sized as-prepared sample (grain size 72 nm). From the result, the 19 nm grain size sample delivered an improved discharge capacity of around 850 mAh/g, whereas it is only 630 mAh/g for as-prepared sample (72 nm). These values are two times higher than that of a carbon anode (372 mAh/g). The anomalous capacity may be associated with the formation of oxygen rich $MgFe_2O_4$ samples.

1. Introduction

In recent decades, transition metal oxides have been extensively investigated as promising anode materials for Li-ion batteries [1–4]. There are two approaches involved in the existing research on anode material, one is improving the electrochemical characteristics of the carbonaceous material by physical or chemical routes, and the other is searching for alternatives to the currently used anode materials. Fe-based compounds have shown much attention for their possible application to Li-ion batteries as electrode materials due to their inexpensive and low toxicity. Among these, spinel Fe_3O_4 has been systematically investigated as lithium intercalation electrodes. However, Sarradin et al. [5] reported that the conventional crystalline iron oxides exhibited poor electro chemical characteristics in terms of electrode capacity and cycleability in the case of micron size particles. Recently, nanosized transition metal oxides (CoO, CuO and NiO) have become attractive alternatives to carbonaceous materials as anode materials in Li-ion batteries because they have twice the capacity per unit mass [1]. For example, Laruelle et al. [6] have found that the oxide CoO exhibits the best performance with reversible capacities as high as 700 mAh/g and good capacity retention for more than 50 cycles. Moreover, Poizot et al. [1] have reported that the electrodes made of nanoparticles of transition-metal oxides (MO, where M: Co, Ni, Cu or Fe) reveal electrochemical capacities of 700 mAh/g with 100% capacity retention for up to 100 cycles and high recharging rate. In addition, Larcher et al. [7] have found that the nanocrystalline α-Fe_2O_3 showed better performance than micron-sized (more than 100 nm) α-Fe_2O_3.

Transition metal oxides MO can react with Fe_2O_3 to form spinel MFe_2O_4. These materials have attracted for their applications in the electronics industries magneto-optic recording devices due to their electrical and magnetic optical properties. Firstly, Chen and Greenblatt [8] have reported that the transition metal ferrites with spinel structure used for cathode materials for Li-ion batteries. Spinel-type ferrite anodes, like $NiFe_2O_4$ [9], $CuFe_2O_4$ [10], $CoFe_2O_4$ [11], $ZnFe_2O_4$ [2] and $CaFe_2O_4$ [12] have gained in significance due to their high specific capacities and simplistic synthesis. The higher capacity observed for the latter materials (i.e. 400–900 mAh/g) compared with graphite (theoretical capacity: 372 mA/g) together with valuable safety feature make these materials an alternative choice as anode. The use of transition-metal nanoparticles to enhance surface electrochemical reactivity will lead to further improvements in the performance of Li-ion batteries [1]. Therefore, wide studies were carried out to search the materials and optimize their performance. Alcántara et al. [13] have reported that $NiFe_2O_4$ powder showed 900 mAh/g reversible capacities in the first cycle with poor cycling performance (400 mAh/g after 10 cycles).

To our knowledge, there have been no reports in the electrochemical behavior on nanocrystalline $MgFe_2O_4$ as anode materials for Li-ion batteries. In the present studies, for the first time, we demonstrate an interesting observation of anomalously high capacity of nano-sized $MgFe_2O_4$ during lithium insertion/deinsertion reactions.

* Corresponding author. Tel.: +82 62 530 1904; fax: +82 62 530 1904.
E-mail address: leeys@chonnam.ac.kr (Y.S. Lee).

0925-8388/$ – see front matter © 2011 Elsevier B.V. All rights reserved.
doi:10.1016/j.jallcom.2011.03.123

2. Experimental

The bulk $MgFe_2O_4$ spinel ferrite has been synthesized by using the ceramic method. Stoichiometry mixtures of powdered reactants containing α-Fe_2O_3 and MgO were thoroughly mixed in the atomic ratio 1:1. The as-prepared sample was milled for 15 h by using planetary high-energy ball mill (Fritsch pulverisette 7) with zirconia vials and balls. The milling speed of vials and balls was 300 rpm with a ball to powder weight ratio of 8:1. The synthesis procedures have been reported elsewhere [14]. The phase analysis for the as-prepared and milled samples was carried out using X-ray diffraction (XRD) with a Rigaku-make high precision Guinier X-ray diffractometer and FeK_α radiation. The average crystalline size was determined from the full width at half maximum of the (3 1 1) reflection of the XRD patterns using Scherrer's formula [15]. The particles sizes and samples internal structures were observed by transmission electron microscopy (TEM, TECNAI, Philips, Netherlands). The specific surface area (S_{BET}, m^2/g) of the samples was measured using Brunauer–Emmett–Teller (BET) surface area analyzer (ASAP 2010 Micromeritics, USA). Thermogravimetric analysis was preformed between 30 and 1000 °C at a rate of 10 °C/min in flowing argon. The working electrode was fabricated with 20.0 mg of $MgFe_2O_4$ powder, 3.0 mg of Ketzen black and 3.0 mg of teflonized acetylene black (TAB), which was pressed on a 200 mm^2 stainless steel mesh, under a pressure of 300 kg/cm^2 and dried at 130 °C for 5 h in an oven. The electrochemical measurements were performed using coin-type CR2032 cells with lithium as anode. A porous polypropylene film (Celgard 3401) was used as the separator and the electrolyte was 1:1 (v/v) ethyl carbonate (EC):dimethyl carbonate (DMC) dissolved in $1MLiPF_6$. The current density of the charge and discharge cycles was 0.2 mA/cm^2 with a cut-off voltage of 5 mV–3.5 V. The electrochemical impedance spectroscopy (EIS) measurement was analyzed within a frequency range of 100 kHz to 0.1 Hz at an open-circuit potential with an a.c. amplitude of 10 mV. Cyclic voltammetry (CV) and EIS were carried out with a Zahner electrochemical unit (1M6e, Zahner, Germany). Galvanostatic charge–discharge cycling of the cells was performed with a battery tester (NAGANO, BTS-2004H, Japan).

3. Results and discussion

The XRD patterns confirmed the presence of spinel phase without any impurity phase for the as-prepared and sintered samples, as reported in our earlier article [14]. The average crystalline sizes were found to be for as-prepared (sample A) and 15 h milled (sample B) samples were 72 and 19 nm respectively, which was determined using Scherrer's formula. The TEM micrographs for sample A and B are shown in Fig. 1(a) and (b), respectively, which shows clearly that the particles are mono-crystalline. The BET surface area of sample A and sample B was determined as 0.13 and 10.76 m^2/g respectively.

The electrochemical impedance spectroscopy is a powerful tool to investigate the capacitive behavior of electrochemical cells of sample A (72 nm), and the sample B (19 nm) $MgFe_2O_4$. Fig. 2 shows typical Nyquist impedance spectra recorded for $MgFe_2O_4$ at a potential of 10 mV within the frequency range of 100 kHz to 0.1 Hz. Both plots consist of one semicircle in high frequency region, which suggests that the contribution to electrical conductivity arises mainly from the grain boundary region, and a straight line in low frequency region. In the high-frequency range, there is a small internal resistance (R_s) at the point intersecting the real axis that may be the ionic resistance of electrolyte, the intrinsic resistance of the active material and current-collector in its interface. In the middle frequency range, the observed semicircle reveals the charge-transfer resistance (R_{ct}), which is 9 Ω for as-prepared and 36 Ω for milled sample. In the low frequency region, both impedance plots exhibit a vertical line due to diffusion processes. In general, the semicircle is associated with the porous structure of the active material and the diameter of the semicircle refers to the polarization resistance. In Fig. 2, it is clear that the polarization resistance is high for milled sample (19 nm) compared with their as-prepared sample (72 nm). If the crystalline size is smaller than the electron mean free path, then the grain boundary scattering becomes dominant, and therefore, the resistance is expected to increase for the smaller crystalline size (milled sample).

The cyclic voltammograms (CVs) of as-prepared (72 nm) and milled (19 nm) $MgFe_2O_4$ samples at scan rate of 0.1 mV s^{-1} between 0 and 3.0 V are shown in Fig. 3. In the case of 72 nm sample, a small

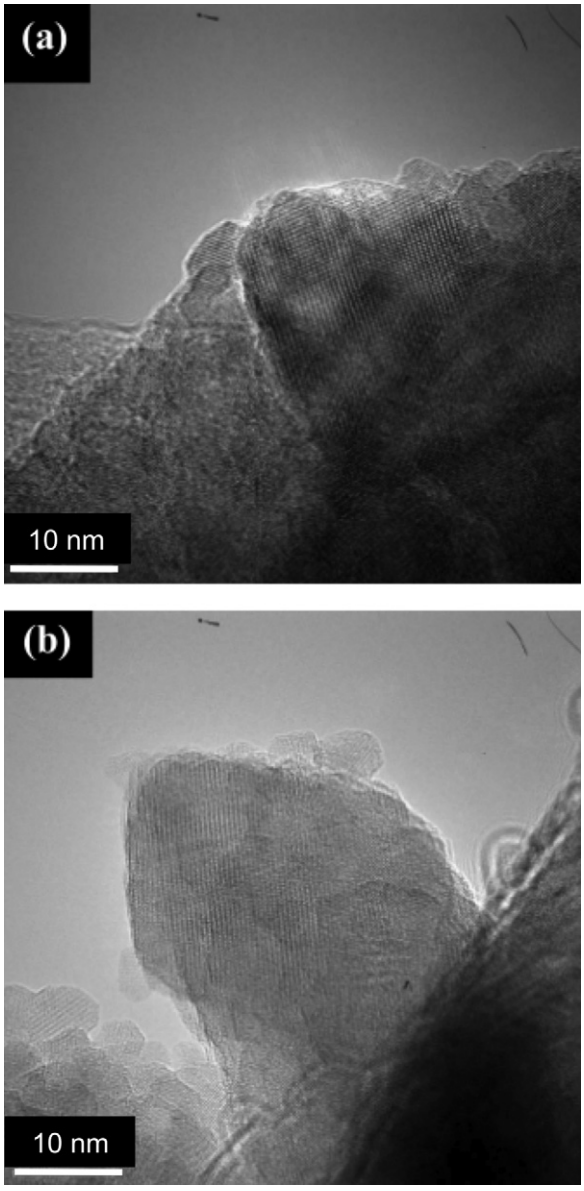

Fig. 1. TEM bright field images of $MgFe_2O_4$ spinel samples: (a) as-prepared and (b) 15 h milled.

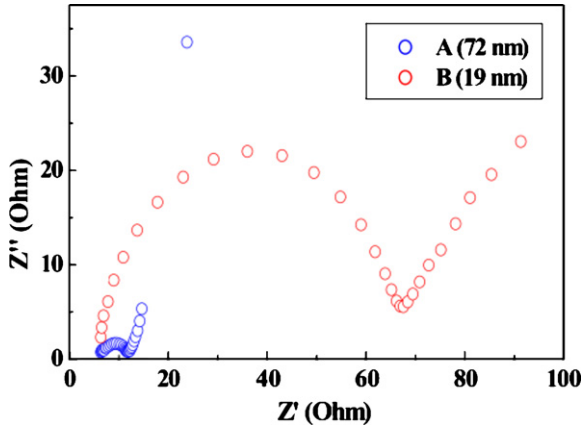

Fig. 2. Nyquist plot of $MgFe_2O_4$ spinel samples: (A) as-prepared and (B) 15 h milled.

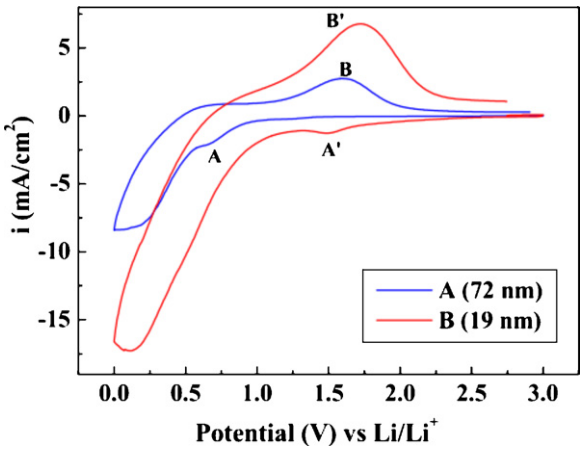

Fig. 3. Galvanostatic cycles of $MgFe_2O_4$ spinel samples: (A) as-prepared and (B) 15 h milled.

cathodic peak A located at 0.7 V is probably associated with the reduction reactions of Fe^{3+} and M^{2+} with Li during the first discharge of MFe_2O_4 material. Larcher et al. [16] have observed that the first discharge plateau of Fe_2O_3 appeared at the same voltage value of 0.7 V. The reduction peak of Fe_2O_3 and MO might be overlapped to form a wide cathodic peak A and A′ under our experimental conditions. The broad anodic peaks B and B′ appears at around 1.59 and 1.72 V for as-prepared and milled samples respectively. These anodic peaks could be attributed due to the oxidation reactions of both metallic Fe and Mg. NuLi and Qin [17] have reported that the anodic peaks are at the same voltage region for $CuFe_2O_4$ and $NiFe_2O_4$ samples.

The first charge–discharge profiles recorded for as-prepared (72 nm) and milled (19 nm) $MgFe_2O_4$ samples at a current density of 0.2 mA cm^{-2} over the voltage region 3.5–0.005 V is presented in Fig. 4. The appearance of two potential plateau around 1.0 and 0.75 V can be attributed to the corresponding reduction of Mg (II) to Mg (0) and Fe(III) to Fe (0) [18]. Normally, two types of mechanisms are superior for the decomposition of MFe_2O_4 anodes, namely: displacive redox mechanism

$$MFe_2O_4 + 8Li^+ + 8e^- \leftrightarrow M + 2Fe + 4Li_2O \quad (1)$$

$$4Li_2O + M + 2Fe \leftrightarrow MO + Fe_2O_3 + 8Li \quad (2)$$

Alloy forming mechanism

$$MFe_2O_4 + 5Li^+ + 5e^- \leftrightarrow Li - M + 2FeO + 2Li_2O \quad (3)$$

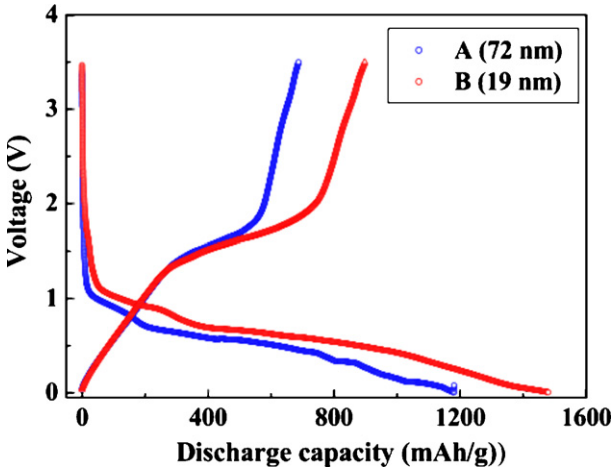

Fig. 4. Initial charge/discharge of $MgFe_2O_4$ spinel samples: (A) as-prepared and (B) 15 h milled sample.

In the present studies, $MgFe_2O_4$ anode samples (A and B) are supposed to follow the displacive redox mechanism due to the observed high specific capacity value of 850 mAh/g. This can be correlated with the comparatively higher Li^+ uptake (~8 Li^+ per formula unit) and higher thermodynamic feasibility of the displacive redox mechanism. Alternatively, an irreversible capacity loss would normally lead in the case of alloy-forming mechanism (Eq. (3)), which is not observed in the present as-prepared and milled $MgFe_2O_4$ anode.

The first-discharge profiles for $MgFe_2O_4$ anode samples (A and B) exhibit a plateau in the range 0.7–0.4 V until capacity of 800–900 mAh/g is reached as shown in Fig. 4. Therefore, the first discharge reaction in the above metal oxides when acting as anode vs. Li is irreversible destruction of the crystal structure that leads to the formation of metal nano-particles embedded in an amorphous matrix of MgO and Li_2O i.e.

$$MgFe_2^{3+}O_4 + 6Li^+ + 6e^- \rightarrow MgO + 2Fe + 3Li_2O \quad (4)$$

On the following charging, in the high voltage range the metal (Fe) particles are covered to oxide together with the decomposition of Li_2O which can be written as

$$Fe + Li_2O \leftrightarrow FeO + 2Li^+ + 2e^- \quad (5)$$

Therefore, cycling proceeds in a reversible three-phase region between metal oxide, Fe and Li_2O. In this, Li_2O is identified to be electrochemically inactive, but in the case of nano-sized metal particles, chemical and physical phenomena be able to effected and the electrochemically driven size confinement of the metal particles is supposed to improve their electrochemical activity towards the formation/decomposition of Li_2O [1,6,19].

During the first discharge to 0 V, a maximum capacity of 1180 mAh/g and 1480 mAh/g were achieved for as-prepared (72 nm) and 15 h milled $MgFe_2O_4$ (19 nm) respectively, whereas the theoretical value is only 1072 mAh/g (8Li_2O per formula). Moreover, these values are almost three times higher than that of a carbon anode (372 mAh/g). The observed extra capacity value establish for the remaining materials can be associated to irreversible reactions with the electrolyte as cell potential approaches 0 V vs. the Li/Li^+ couple [13]. Also, this may be explained partly on the basis of reversible formation of polymeric gel layer around the metal nano-particles as observed with 3d metal oxides [6]. Similar high discharge capacity values were reported previously than the theoretical value for transition metal oxide materials [12,13].

From Fig. 4, it can be clearly seen that the 15 h milled sample (19 nm) has higher capacity value than that of as-prepared sample (72 nm). The reason for higher capacity of milled sample should basically be attributed to the smaller size with larger surface area than their as-prepared sample. Thus, the milled sample can provide more reaction sites on the surface and the smaller diameter provides a short diffusion length for Li diffusion, which could improve the charge transfer and the electrochemical reactions [20]. Moreover, decrease in mean particle size results in an increase in cyclability and rate capacity of cathode materials since smaller particles are more flexible for lithium insertion–deinsertion than larger particles [21]. As, the capacity obtained for milled sample (19 nm) is 27% higher than expected theoretical capacity, therefore the amount of anomalous capacity may be related to the participation of excess oxygen in the electrochemical behavior [19]. To confirm this assumption, thermogravimetric (TGA) measurements were carried out on as-prepared (72 nm) and 15 h milled (19 nm) samples (Fig. 5). In Fig. 5, the first weight loss at around 375 °C, and the second weight loss between 600 and 780 °C are due to dehydration and decomposition of excess oxygen on $MgFe_2O_4$ surface, respectively. The cycling performances of the samples are shown in Fig. 6. It should be noted that, the maximum reversible capacity value is affected by a marked decrease during first cycles,

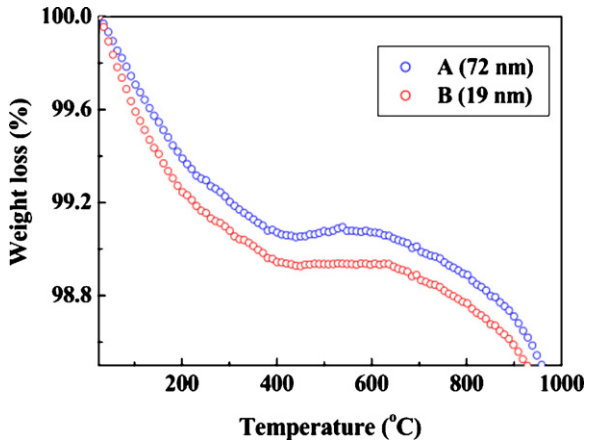

Fig. 5. TGA curves of $MgFe_2O_4$ spinel samples: (A) as-prepared and (B) 15 h milled sample.

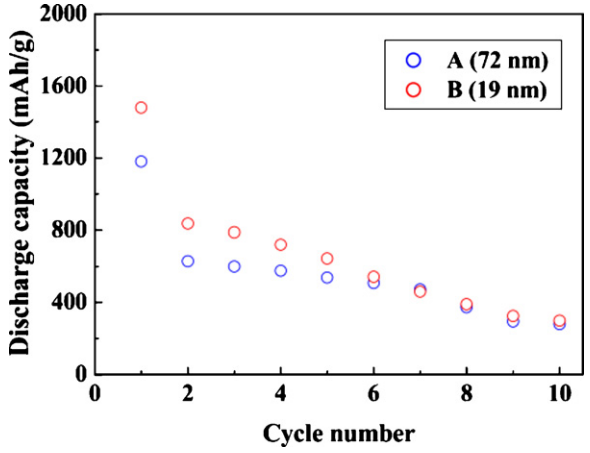

Fig. 6. Cyclic performance of $MgFe_2O_4$ spinel samples: (A) as-prepared and (B) 15 h milled sample.

stabilizing at 300 mAh/g after ten cycles, which is the drawback of these potential candidates for the negative electrode of lithium ion cells.

4. Conclusions

Nanostructured $MgFe_2O_4$ powders have been prepared by solid state route with the grain size of 72 nm. The grain size was further reduced to 19 nm by milling the as-prepared sample. In this study, the anomalously high capacity has been investigated in nanocrystalline $MgFe_2O_4$ anode material. This is the first time that this $MgFe_2O_4$ is used as active electrode material vs. lithium metal in the test cell. A first discharge capacity of 1480 mAh/g has been observed in the milled $MgFe_2O_4$ sample, whereas it is only 1180 mAh/g for as-prepared sample (72 nm). This value is three times higher than that of a carbon anode (372 mAh/g). From these results, we suggested that the improved electrochemical performance of milled $MgFe_2O_4$ electrode might from the effect of grain size on their electrochemical properties.

Acknowledgements

This work was supported by Priority Research Centers Program through the National Research Foundation of Korea (NRF) funded by the Ministry of Education, Science and Technology (2010-0029626).

References

[1] P. Poizot, S. Laruelle, S. Grugeon, L. Dupont, J.-M. Tarascon, Nature 407 (2000) 496.
[2] Y.N. NuLi, Y.Q. Chu, Q.Z. Qin, J. Electrochem. Soc. 151 (2004) A1077.
[3] R. Kalai Selvan, N. Kalaiselvi, C.O. Augustin, C.H. Doh, C. Sanjeeviraja, J. Power Sources 157 (2006) 522.
[4] L.F. Nazar, G. Goward, F. Leroux, M. Duncan, H. Huang, T. Kerr, J. Gaubicher, Int. J. Inorg. Mater. 3 (2001) 191.
[5] J. Sarradin, A. Guessous, M. Ribes, J. Power Sources 62 (1996) 149.
[6] S. Laruelle, S. Grugeon, P. Poizot, M. Dollé, L. Dupont, J.-M. Tarascon, J. Electrochem. Soc. 149 (2002) A627.
[7] D. Larcher, C. Masquelier, D. Bonnie, Y. Chabre, V. Masson, J.B. Leriche, J.-M. Tarascon, J. Electrochem. Soc. 150 (2003) A133.
[8] C.J. Chen, M. Greenblatt, Solid State Ionics 18–19 (1986) 838.
[9] X.D. Li, W.S. Yang, F. Li, D.G. Evans, X. Duan, J. Phys. Chem. Solids 67 (2006) 1286.
[10] M. Bomio, P. Lavela, J.L. Tirado, ChemPhysChem 8 (2007) 1999.
[11] Y.-Q. Chu, Z.-W. Fu, Q.-Z. Qin, Electrochim. Acta 49 (2004) 4915.
[12] N. Sharma, K.M. Shaju, G.V. Subba Rao, B.V.R. Chowdari, J. Power Sources 124 (2003) 204.
[13] R. Alcántara, M. Jarana, P. Lavela, J.L. Tirado, J.C. Jumas, J. Olivier-Fourcade, Electrochem. Commun. 5 (2003) 16.
[14] N. Sivakumar, A. Narayanasamy, J.-M. Greneche, R. Murugaraj, Y.S. Lee, J. Alloys Compd. 504 (2010) 395.
[15] B.D. Cullity, Elements of X-ray Diffraction, Addison Wesley, CA, 1978.
[16] D. Larcher, C. Masquelier, D. Bonnin, Y. Chabre, V. Masson, J.B. Leriche, J.-M. Tarascon, J. Electrochem. Soc. 150 (2003) A133.
[17] Y.N. NuLi, Q.Z. Qin, J. Power Sources 142 (2005) 292.
[18] X. Yang, X. Wang, Z. Zhang, J. Crystal Growth 277 (2005) 463.
[19] G.X. Wang, Y. Chen, K. Konstantinov, M. Lindsay, H.K. Liu, S.X. Dou, J. Power Sources 109 (2002) 142.
[20] C.H. Chen, B.J. Hwang, J.S. Do, J.H. Weng, M. Venkateswarlu, M.Y. Cheng, R. Santhanam, K. Ragavendran, J.F. Lee, J.M. Chen, D.G. Liu, Electrochem. Commun. 12 (2010) 496.
[21] V. Manev, W. Ebner, W. Thompson, S. Dow, US pat. 5,961,949, 1999.